# Synthesis, Crystal Structure and Density Functional Calculations on 1-Phenyl-3-*p*-fluorophenyl-5-*p*-chlorophenyl-2-pyrazoline

**Pu Su Zhao, Yu Feng Li, Huan Mei Guo,† Fang Fang Jian,* and Xian Wang**

*New Materials & Function Coordination Chemistry Laboratory, Qingdao University of Science and Technology, Qingdao Shandong 266042, P.R. China. *E-mail: zhaopusu@163.com*
*†Department of Chemistry, Weifang University, Weifang Shandong 261061, P.R. China*
*Received May 18, 2007*

1-Phenyl-3-*p*-fluorophenyl-5-*p*-chlorophenyl-2-pyrazoline has been synthesized and characterized by elemental analysis, IR, UV-Vis and X-ray single crystal diffraction. Density functional calculations show that B3LYP/6-311G** method can reproduce the structural parameters. The electronic absorption spectra have been predicted based on the optimized structure by using 6-311G** and 6-311++G** basis sets and compared with the experimental values. The results indicate that TD-DFT method can only predict the electronic absorption spectra of the system studied here approximately. On the basis of vibrational analyses, the thermodynamic properties of the title compound at different temperatures have been calculated, revealing the correlations between $C_{p,m}^0$, $S_m^0$, $H_m^0$ and temperature.

**Key Words :** Synthesis, Crystal structure, Density functional calculations, Electronic absorption spectra, Thermodynamic property

## Introduction

In general, fluorinated compounds are the focus of much interest in modern chemistry and are ideal for use in drug design because of their good biological activities.[1-4] On the other hand, fluorescent probes are powerful tools in cell biology for the non-invasive measurement of intracellular ion concentrations.[5] They have found widespread applications, for example, to gauge intracellular calcium concentrations,[6] to visualize labile zinc[7,8] and iron pools.[9] Among various possible fluorescent probes, pyrazoline-based fluorophores stand out due to their simple structure and favorable photophysical properties such as large extinction coefficient and quantum yields ($\Phi_f \approx 0.6$-$0.8$).[10] Their attractive properties, including cation- or pH-sensitive probes, have been described,[11] and the suitability of pyrazoline fluorophores as probes in a biological environment is also explored.[12] These facts prompted us to synthesize pyrazoline-based fluorophores containing fluorophenyl substituted group, which might be expected to have both good biological activities and fluorescent properties. Herein, we wish to report the crystal structure of 1-phenyl-3-*p*-fluorophenyl-5-*p*-chlorophenyl-2-pyrazoline as well as its synthesis and characterizations. At the same time, we wish to give reports about the theoretical calculations by using B3LYP method. These information will provide important information for the further study on the activities and fluorescent properties of the title compound, which are in progress.

## Experimental Section and Calculational Method

**Physical measurements.** Elemental analyses for carbon, hydrogen and nitrogen were performed by a Perkin-Elmer 240C elemental instrument. The melting points were determined on a Yanaco MP-500 melting point apparatus. The IR spectra were recorded in the range of 4000-400 $cm^{-1}$ using KBr pellets on a Nicolet 170SX spectrophotometer. Electronic absorption spectra were measured on a Shimadzu UV3100 spectrophotometer in hexahydrobenzene solution.

**Synthesis.** All chemicals were obtained from a commercial source and used without further purification.

The reaction path is shown in Scheme 1.

1-*p*-Fluorophenyl-3-*p*-chlorophenyl-2-propenyl-1-ketone (0.01 mol) and phenylhydrazine (0.015 mol) were mixed in acetic acid (40 mL) and stirred in refluxing for 6 h, then, the mixture was poured into ice-water to afford light-yellow solids. The solids were filtrated and washed with water until the pH of solution is about to 7. Finally, the yellow solid crystals were dry under room temperature. Yield 85%. mp. 149-150 °C. IR: $\nu$ 3042 (m), 2914(m), 1885(w), 1649(w), 1593(vs), 1567(s), 1513(s), 1489(vs), 1410(s), 1383(vs), 1317(vs), 1285(s), 1231(vs), 1152(m), 1118(vs), 1106(vs), 1067(s), 1014(m), 953(m), 832(vs), 809(s), 742(vs), 689 (vs), 615(s), 512(s) $cm^{-1}$. Found: C, 71.78; H, 4.48; N, 7.80%. Calc. for $C_{21}H_{16}ClFN_2$: C, 71.89; H, 4.60; N, 7.99.

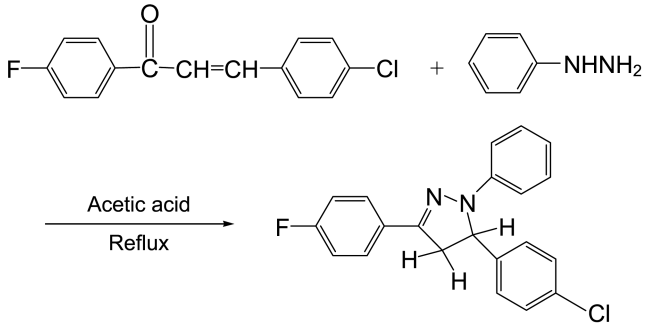


**Scheme 1**

**Table 1**. Crystal data and structure refinement

| | |
|---|---|
| Empirical formula | $C_{21}H_{16}ClFN_2$ |
| Formula weight | 350.81 |
| Temperature | 293(2) K |
| Wavelength | 0.71073 Å |
| Crystal system, space group | Monoclinic, *P*21/*c* |
| Unit cell dimensions | $a$ = 20.286(4) Å |
| | $b$ = 5.3827(11)Å $\beta$ =104.95(3)° |
| | $c$ = 16.254(3) Å |
| Volume | 1714.7(6) Å$^3$ |
| *Z*, Calculated density | 4, 1.359 Mg/m$^3$ |
| Absorption coefficient | 0.238 |
| *F*(000) | 728 |
| $\theta$ range for data collection | 2.08 to 25.00 ° |
| Limiting indices | $-24 \le h \le 22$, $-6 \le k \le 6$, $-19 \le l \le 16$ |
| Reflections collected/unique | 6705 / 3018 [$R_{int}$ = 0.0186] |
| Refinement method | Full-matrix least-squares on $F^2$ |
| Data / restraints / parameters | 3018 / 0 / 226 |
| Goodness-of-fit on $F^2$ | 1.069 |
| Final $R$ indices [$I > 2\sigma(I)$] | $R_1$ = 0.0673, $wR_2$ = 0.1514 |
| $R$ indices (all data) | $R_1$ = 0.0785, $wR_2$ = 0.1584 |
| Largest diff. peak and hole | 0.345 and −0.379 e. Å$^{-3}$ |

Electronic absorption spectra in hexahydrobenzene (nm, log $\varepsilon$): $\lambda$ = 211 (1.68), $\lambda_{max}$ = 223 (1.80), $\lambda$ = 354 (1.61).

**Crystal structure determination.** The diffraction data were collected on a Enraf-Nonius CAD-4 diffractometer with graphite- monchromated *Mo-K*$\alpha$ radiation ($\lambda$ = 0.71073 Å, $T$ = 293 K). The technique used was $\omega$-scan with limits 2.08 to 25.00°. The structure of the title compound was solved by direct method and refined by least squares on $F^2$ by using the *SHELXTL*[13] software package. All non-hydrogen atoms were anisotropically refined. The hydrogen atom positions were fixed geometrically at calculated distances and allowed to ride on the parent carbon atoms. The final conventional $R$ = 0.0673 and $R_w$ = 0.1514 for 2540 reflections with $I > 2\sigma(I)$ using the weighting scheme, $w = 1/[\sigma^2(F_o^2) + (0.0554\,P)^2 + 1.6627\,P]$, where $P = (F_o^2 + 2F_c^2)/3$. The molecular graphics were plotted using *SHELXTL*. Atomic scattering factors and anomalous dispersion corrections were taken from *International Tables for X-ray Crystallography*.[14] A summary of the key crystallographic information is given in Table 1.

**Computational methods.** The crystal structure of the title compound was used as initial molecular geometry, then it was optimized by using MM+ molecular modeling and semi-empirical AM1 mehtod[15] (HYPERCHEM 6.0, Hypercube, Ont., Canada). In the next step, B3LYP (Becke's three parameter hybrid functional using the LYP correlation functional) calculations at basis set 6-311G** by the Berny method[16] were performed with the Gaussian 03 software package.[17] Vibrational frequencies calculated ascertain the structure was stable (no imaginary frequencies). The thermodynamic properties of the title compound at different temperatures were calculated on the basis of vibrational analyses. Electronic absorption spectra were calculated by using time-dependent density functional theory (TD-DFT)[18-20] method at 6-311G** and 6-311++G** basis sets, respectively. Natural Bond Orbital (NBO) analyses were performed on the optimized structures.[21]

All calculations were performed on a DELL PE 2850 server and a Pentium IV computer using the default convergence criteria.

## Results and Discussion

**Description of the crystal structure.** Single crystal suitable for X-ray measurements was obtained by recrystallization from acetic ether at room temperature.

The displacement ellipsoid plot with the numbering scheme for the title compound is shown in Figure 1. Figure 2 shows a perspective view of the crystal packing in the unit cell. Selected bond lengths, bond angles and torsion angles by X-ray diffractions are listed in Table 2 along with the calculated bond parameters.

X-ray single crystal structure determination indicates the molecular structure consists of discrete [$PhFC_3H_3N_2PhPhCl$] units, which are connected together by crystal-field interactions. All of the bond lengths and bond angles in the phenyl rings are in the normal range. In the pyrazolinyl ring,

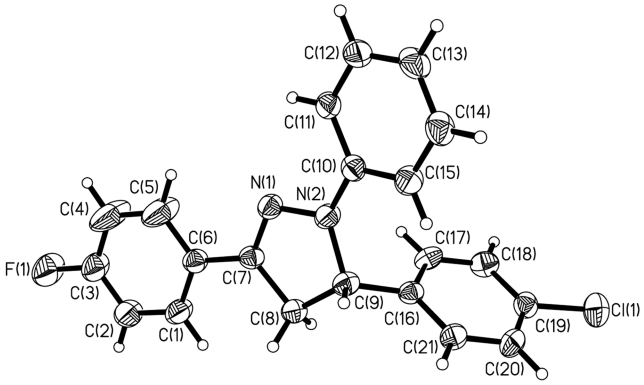


**Figure 1**. The molecular structure with the atomic numbering for the title compound.

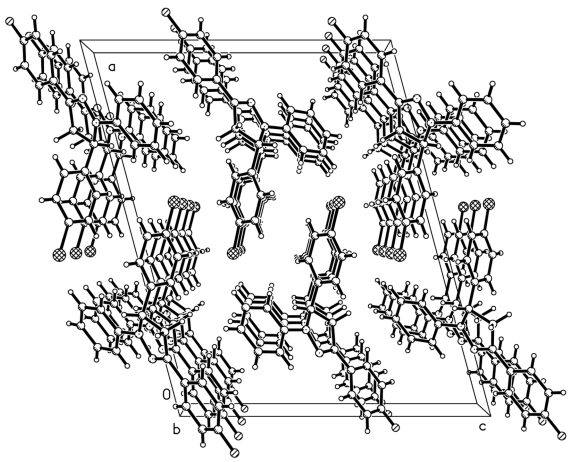


**Figure 2**. Packing diagram of the unit cell along the *b*-axial for the title compound.

**Table 2**. Selected structural parameters by X-ray and theoretical calculations

| Bond lengths (Å) | Exp. | Calc. | Bond lengths (Å) | Exp. | Calc. |
|---|---|---|---|---|---|
| F(1)-C(3) | 1.355(4) | 1.351 | C(3)-C(4) | 1.330(6) | 1.390 |
| N(1)-C(7) | 1.280(4) | 1.289 | C(5)-C(6) | 1.357(5) | 1.408 |
| N(1)-N(2) | 1.375(3) | 1.364 | C(6)-C(7) | 1.464(4) | 1.462 |
| N(2)-C(9) | 1.476(4) | 1.478 | C(9)-C(16) | 1.512(4) | 1.521 |
| N(2)-C(10) | 1.394(4) | 1.398 | C(10)-C(15) | 1.388(4) | 1.404 |
| Cl(1)-C(19) | 1.742(3) | 1.760 | C(12)-C(13) | 1.377(5) | 1.395 |
| C(7)-C(8) | 1.500(4) | 1.517 | C(14)-C(15) | 1.376(4) | 1.392 |
| C(8)-C(9) | 1.538(4) | 1.555 | C(16)-C(21) | 1.376(4) | 1.397 |
| C(1)-C(2) | 1.385(5) | 1.392 | C(18)-C(19) | 1.369(4) | 1.391 |
| | | | C(19)-C(20) | 1.370(5) | 1.390 |
| **Bond angles (º)** | **Exp.** | **Calc.** | **Bond angles (º)** | **Exp.** | **Calc.** |
| C(7)-N(1)-N(2) | 109.3(2) | 110.4 | N(2)-C(9)-C(8) | 101.3(2) | 101.7 |
| N(1)-N(2)-C(9) | 112.7(2) | 112.9 | C(15)-C(10)-C(11) | 118.7(3) | 118.9 |
| C(6)-C(1)-C(2) | 121.7(3) | 121.2 | C(14)-C(13)-C(12) | 118.9(3) | 118.8 |
| C(2)-C(3)-C(4) | 121.1(4) | 121.9 | C(13)-C(14)-C(15) | 121.0(3) | 121.0 |
| C(2)-C(3)-F(1) | 119.4(3) | 119.2 | C(21)-C(16)-C(17) | 118.2(3) | 118.8 |
| C(1)-C(6)-C(7) | 122.0(3) | 120.7 | C(18)-C(19)-C(20) | 121.1(3) | 121.0 |
| N(1)-C(7)-C(8) | 113.4(2) | 112.7 | C(18)-C(19)-Cl(1) | 119.0(3) | 119.5 |
| C(7)-C(8)-C(9) | 102.8(2) | 102.3 | C(16)-C(21)-C(20) | 121.1(3) | 121.2 |
| **Torsion angles (º)** | **Exp.** | **Calc.** | **Torsion angles (º)** | **Exp.** | **Calc.** |
| N(1)-N(2)-C(10)-C(11) | –15.24 | –5.74 | N(1)-C(7)-C(6)-C(1) | 177.34 | 177.98 |
| N(1)-N(2)-C(10)-C(15) | 167.30 | 174.56 | N(1)-C(7)-C(6)-C(5) | 0.06 | 1.746 |
| C(9)-N(2)-C(10)-C(15) | 8.21 | 10.46 | C(8)-C(7)-C(6)-C(1) | –3.75 | 1.503 |
| N(2)-C(9)-C(16)-C(17) | –40.90 | –31.84 | N(2)-C(9)-C(16)-C(17) | 73.76 | 83.71 |
| N(2)-C(9)-C(16)-C(21) | 139.42 | 150.85 | | | |

**Table 3**. C-H$\cdots\pi$ supramolecular interactions

| D-H$\cdots$A | Symmetry | D$\cdots$A (Å) | $\angle$D-H$\cdots$A (°) |
|---|---|---|---|
| C(1)-H(1B)$\cdots$Cg(3) [C(10)-C(15)] | *X*, 1/2–*Y*, 1/2+*Z* | 3.906 | 127.08 |
| C(9)-H(9A)$\cdots$Cg(3) [C(10)-C(15)] | *X*, 1+*Y*, *Z* | 3.592 | 152.46 |

the C=N bond lengths are shorter than those found in similar structures.[22-25] The bond lengths of N-N and C-N are corresponding to those found in the above-cited structures.[22-24] The dihedral angles between the pyrazolinyl ring and the phenyl rings at positions 1, 3 and 5 of the pyrazoline are 8.87(2), 3.87(2) and 76.51(2)°, respectively.

In the crystal lattice, there exist some C-H$\cdots\pi$ supramolecular interactions[25] (see Table 3 and Figure 3). On the other hand, there is one type of $\pi\cdots\pi$ stacking interaction[26] between pyrazolinyl ring (*X*, *Y*, *Z*) and phenyl ring [C(16)-C(21)] (*X*, *Y*, *Z*), with the center-to-center distance and the shortest interplanar distance being 3.883 Å and 2.065 Å, respectively. All above intermolecular interactions stabilize the crystal structures in the solid state.

**Geometric optimization.** B3LYP/6-311G** theoretical calculations are carried out, and the optimized parameters are also listed in Table 2. Most of the optimized bond lengths are slightly larger than the experimental values, since that the theoretical calculations belong to isolated molecules in gaseous phase and the experimental results belong to molecules in solid state. The biggest deviation of bond

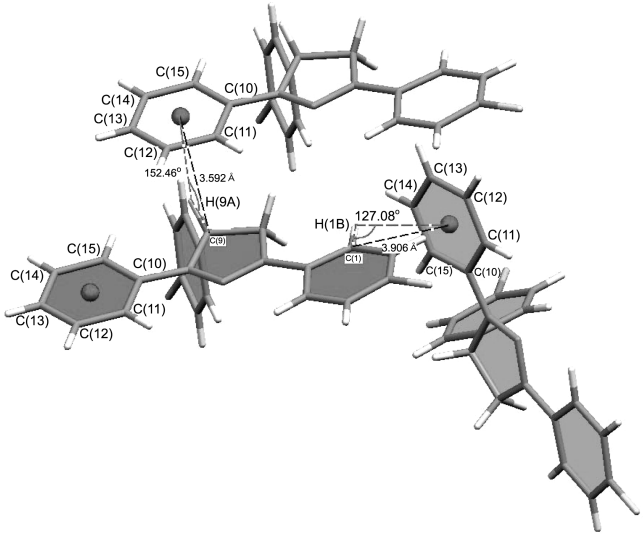


**Figure 3**. C-H$\cdots\pi$ supramolecular interactions ( red dots denote the centroids of phenyl rings of C(10)-C(15), respectively. For clarity purpose, only bonds of C(1)-H(1B) and C(9)-H(9A) are presented).

length and bond angle are 0.060 Å at C(3)-C(4) bond and 1.3° at C(1)-C(6)-C(7) bond angle, respectively. In addition, the existences of the crystal field and intramolecuar interactions also result in the difference of torsion angles between the experimental values and theoretical ones, with the biggest difference being 11.43° at N(2)-C(9)-C(16)-C(21). Although there are differences between the experimental structural parameters and theoretical values, the optimized geometry reproduces the most strucutural information of the title compound, which suggest that B3LYP/6-311G** method is suitable for investigating the system studied here. Based on the optimized geometry, electronic spectra and thermodynamic properties are calculated as we described below.

**Electronic absorption spectra.** Based on the B3LYP/6-311G** level optimized geometry, electronic absorption spectra were calculated by using TD-DFT method with 6-311G** and 6-311++G** basis sets respectively. Experimental electronic absorption spectra values along with theoretical electronic absorption spectra information are all given in Table 4. In view of peak positions and peak numbers, experimental electronic absorption spectra have three transition bands , while both the theoretical electronic spectra calculated with two basis sets give four absorption bands, with three being acute peaks and one being shoulder peak (239-241 nm/244-246 nm). Compared with the experimental values, the theoretical spectra values calculated with 6-311G** basis set give small differences in short wavelengths range, such as from 210-221 nm, while the spectra values calculated with 6-311++G** basis set give small differences at longer wavelength, such as 356 nm. As for the peak intensity, in the experimental spectra, the strongest peak is observed at 223 nm, while in the theoretical spectra, the strongest one appears at 347 nm by using TDDFT/B3LYP/6-311G** level and 356 nm by using TDDFT/B3LYP/6-311++G** level, respectively. Namely, for the system studied here, with 6-311G** and 6-311++G** basis sets, TD-DFT method can only predict electronic absorption spectra approximately. The reason for the discrepancy between the experimental values and theoretical predictions may be as follows: TD-DFT approach is based on the random-phase approximation (RPA) method,[27-28] which provides an alternative to computationally demanding multi-refrence configuration interaction methods in the study of excited states. TD-DFT calculations do not evaluate the spin-orbit splitting; the values are averaged. Here, in our

**Table 4**. Experimental and theoretical electronic absorption spectra values

| Exp. | | Cal. 6-311G** | | | Cal. 6-311++G** | | |
|---|---|---|---|---|---|---|---|
| wave length (nm) | log $\delta$ | wave length (nm) | oscillator strength | Transition | wave length (nm) | oscillator strength | Transition |
| 211 | 1.68 | 210 | 0.1026 | HOMO-3 → LUMO+2 | 205 | 0.0869 | HOMO-3 → LUMO+3 |
| 223 | 1.80 | 221 | 0.1639 | HOMO-2 → LUMO+1 | 227 | 0.1058 | HOMO-2 → LUMO+1 |
| | | | | HOMO-3 → LUMO | | | HOMO-1 → LUMO+2 |
| | | 239 | 0.1490 | HOMO-3 → LUMO | 244 | 0.1063 | HOMO-3 → LUMO |
| | | 241 | 0.1785 | HOMO-2 → LUMO | 246 | 0.1860 | HOMO-2 → LUMO |
| | | | | HOMO-1 → LUMO | | | HOMO-1 → LUMO |
| 354 | 1.61 | 347 | 0.4166 | HOMO → LUMO | 356 | 0.3999 | HOMO → LUMO |

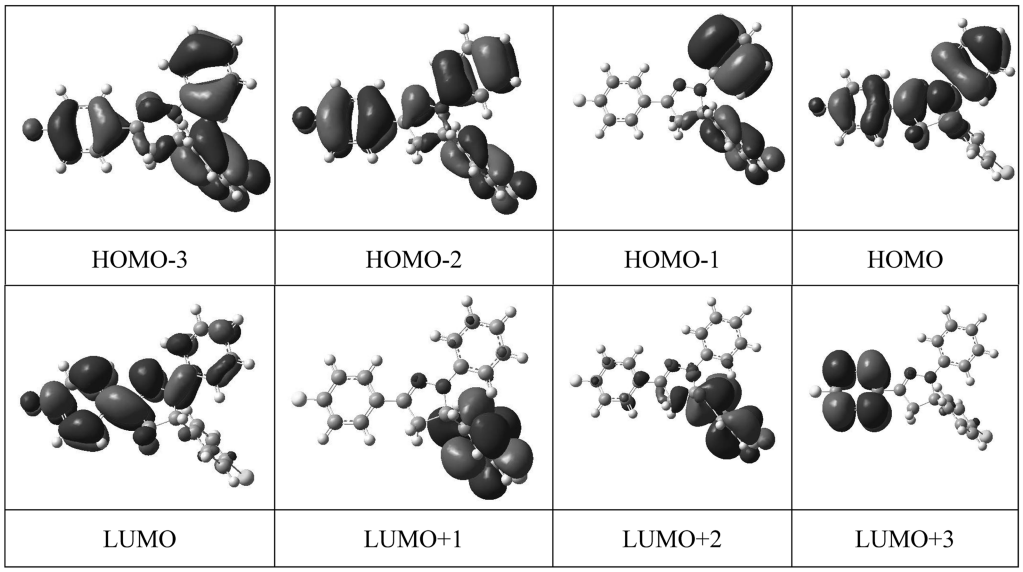


**Figure 4**. Molecular obtials active in the electronic transitions of the title compound.

**Table 5**. Thermodynamic properties of the title compound at different temperatures

| $T$ (K) | $C^0_{p,m}$ (J·mol$^{-1}$·K$^{-1}$) | $S^0_m$ (J·mol$^{-1}$·K$^{-1}$) | $H^0_m$ (kJ·mol$^{-1}$) |
|---|---|---|---|
| 100.0 | 140.72 | 418.93 | 9.34 |
| 200.0 | 242.63 | 546.52 | 28.33 |
| 298.1 | 356.10 | 664.43 | 57.68 |
| 300.0 | 358.23 | 666.64 | 58.35 |
| 400.0 | 466.11 | 784.86 | 99.70 |
| 500.0 | 554.89 | 898.78 | 150.92 |
| 600.0 | 625.04 | 1006.40 | 210.05 |

paper, the objective is to evaluate the electronic structure by direct electronic excitations. Only singlet-singlet transitions are considered in these quasi-relativistic calculations. In addition, the role of the solvent effect of hexahydrobenzene solution is not included in the theoretical calculations. The detailed electronic transition modes corresponding to each absorption peak are also listed in Table 4. Based on the optimized structures, molecular orbital coefficients analyses indicate that the frontier molecular orbitals are mainly composed of $p_y$ and $p_z$ atomic orbitals and electronic absorption spectra aforementioned are mainly assigned to $n$-$\pi^*$ and $\pi$-$\pi^*$ electron transitions. Some frontier molecular orbitals surfaces of the title compound are showed in Figure 4.

**Thermodynamic properties.** On the basis of statistical thermodynamic and vibrational analysis at B3LYP/6-311G** level, the standard thermodynamic functions: heat capacity ($C^0_{p,m}$), entropy ($S^0_m$) and enthalpy ($H^0_m$) were obtained and listed in Table 5. The scale factor for the frequencies is 0.96.

As observed from Table 5, all the values of $C^0_{p,m}$, $S^0_m$ and $H^0_m$ increase with the increase of temperature from 100.0 to 600.0 K, which is attributed to the enhancement of the molecular vibration while the temperature increases.

The correlations linear equations between these thermodynamic properties and temperatures $T$ are as follows:

$$C^0_{p,m} = 7.8255 + 1.3127\,T - 4.5953 \times 10^{-4}\,T^2$$
$$S^0_m = 288.5842 + 1.3279\,T - 2.1825 \times 10^{-4}\,T^2$$
$$H^0_m = -0.7142 + 4.4506 \times 10^{-2}\,T + 5.1322 \times 10^{-4}\,T^2$$

These equations could be used for the further studies of the title compound. For instance, when we investigate the interactions between the title compound and another compound, thermodynamic properties $S^0_m$ and $H^0_m$ could be obtained from these equations and then used to calculate the change of Gibbs free energy of the reaction, which will assist us to judge the spontaneity of the reaction.

## Conclusions

1-Phenyl-3-*p*-fluorophenyl-5-*p*-chlorophenyl-2-pyrazoline has been synthesized by the reaction of phenylhydrazine and the derivative of chalcone and its crystal structure also has been obtained. B3LYP/6-311G** calculations show that optimized geometry resemble the crystal structure closely. For the system studied here, TD-DFT method can only predict electronic absorption spectra approximately. Thermodynamic properties at different temperatures have been calculated and the correlations between these thermodynamic properties and temperatures $T$ are also obtained.

**Supplementary data.** Crystallographic data for the structure reported here have been deposited with Cambridge Crystallographic Data Center (Deposition No. CCDC-626448). The data can be obtained free of charge via www.ccdc.cam.ac.uk/conts/retrieving.html (or from the CCDC, 12 Union Road, Cambridge CB2 1EZ, UK; fax: +44 1223 336033; e-mail: deposit@ccdc.cam.ac.uk).

**Acknowledgment.** This work was supported by Natural Science Foundation of Shandong Province (No. Y2005B04), P. R. China, Doctoral Fund of Shandong Province, P. R. China, (No. 2006BS01043) and Doctoral Fund of Qingdao University of Science & Technology.

## References

1. Shi, W.; Qian, X. H.; Song, G. H.; Zhang, R.; Li, R. P. *J. Fluor. Chem*. **2000**, *106*, 173.
2. Ogunbadeniyi, A. M.; Adejare, A. *J. Fluor. Chem.* **2002**, *114*, 39.
3. O'Hagan, D.; Rzepa, R. S. *Chem. Commun*. **1997**, 645.
4. Welch, J. T. *Tetrahedron*. **1982**, *38*, 871.
5. Mason, W. T. *Fluorescent and Luminescent Probes for Biological Activity: A Practical Guide to Technology for QuantitatiVe Real-time Analysis*; Academic Press: San Diego, CA, 1999.
6. Takahashi, A.; Camacho, P.; Lechleiter, J. D.; Herman, B. *Physiol. Rev.* **1999**, *79*, 1089.
7. Burdette, S. C.; Walkup, G. K.; Spingler, B.; Tsien, R. Y.; Lippard, S. J. *J. Am. Chem. Soc*. **2001**, *123*, 7831.
8. Hirano, T.; Kikuchi, K.; Urano, Y.; Nagano, T. *J. Am. Chem. Soc*. **2002**, *124*, 6555.
9. Esposito, B. P.; Epsztejn, S.; Breuer, W.; Cabantchik, Z. I. *Anal. Biochem.* **2002**, *304*, 1.
10. Rivett, D. E.; Rosevear, J.; Wilshire, J. F. K. *Aust. J. Chem*. **1983**, *36*, 1649.
11. Rurack, K.; Resch-Genger, U.; Bricks, J. L.; Spieles, M. *Chem. Commun*. **2000**, 2103.
12. Fahrni, C. J.; Yang, L. C.; VanDerveer, D. G. *J. Am. Chem. Soc*. **2003**, *125*, 3799.
13. Sheldrick, G. M. *SHELXTL, v5 Reference Manual*; Siemens Analytical X-Ray Systems: Madison, WI, 1997.
14. Wilson, A. J. *International Table for X-Ray Crystallography*; Kluwer Academic: Dordrecht, The Netherlands, 1992; Vol. C: Tables 6.1.1.4 (pp 500-502) and 4.2.6.8 (pp 219-222), respectively.
15. Dewar, M. J. S.; Zoebisch, E. G.; Healy, E. F. *J. Am. Chem. Soc*. **1985**, *107*, 3902.
16. Peng, C.; Ayala, P. Y.; Schlegel, H. B.; Frisch, M. J. *J. Comput. Chem*. **1996**, *49*, 17.
17. Frisch, M. J.; Trucks, G. W.; Schlegel, H. B.; Scuseria, G. E.; Robb, M. A.; Cheeseman, J. R.; Montgomery, J. A.; Vreven, Jr., T.; Kudin, K. N.; Burant, J. C.; Millam, J. M.; Iyengar, S. S.; Tomasi, J.; Barone, V.; Mennucci, B.; Cossi, M.; Scalmani, G.; Rega, N.; Petersson, G. A.; Nakatsuji, H.; Hada, M.; Ehara, M.; Toyota, K.; Fukuda, R.; Hasegawa, J.; Ishida, M.; Nakajima, T.; Honda, Y.; Kitao, O.; Nakai, H.; Klene, M.; Li, X.; Knox, J. E.; Hratchian, H. P.; Cross, J. B.; Adamo, C.; Jaramillo, J.; Gomperts, R.; Stratmann, R. E.; Yazyev, O.; Austin, A. J.; Cammi, R.; Pomelli, C.; Ochterski, J. W.; Ayala, P. Y.; Morokuma, K.; Voth,

G. A.; Salvador, P.; Dannenberg, J. J.; Zakrzewski, V. G.; Dapprich, S.; Daniels, A. D.; Strain, M. C.; Farkas, O.; Malick, D. K.; Rabuck, A. D.; Raghavachari, K.; Foresman, J. B.; Ortiz, J. V.; Cui, Q.; Baboul, A. G.; Clifford, S.; Cioslowski, J.; Stefanov, B. B.; Liu, G.; Liashenko, A.; Piskorz, P.; Komaromi, I.; Martin, R. L.; Fox, D. J.; Keith, T.; Al-Laham, M. A.; Peng, C. Y.; Nanayakkara, A.; Challacombe, M.; Gill, P. M. W.; Johnson, B.; Chen, W.; Wong, M. W.; Gonzalez, C.; Pople, J. A. Gaussian, Inc.: Wallingford, CT, 2004.

18. Petersilka, M.; Gossmann, U. J.; Gross, E. K. U. *Phys. Rev. Lett.* **1966**, *76*,1212.
19. Bauernschmitt, R.; Ahlrichs, R. *Chem. Phys. Lett.* **1996**, *256*, 1996.
20. Jamorski, C.; Casida, M. E.; Salahub, D. R. *J .Chem. Phys.* **1996**, *104*, 5134.
21. Runge, E.; Gross, E. K. U. *Phys. Rev. Lett.* **1984,** *52*, 997.
22. Guo, H. M.; Jian, F. F.; Zhou, L. Y.; Zhao, P. S.; Zheng, J. *Acta Cryst.* **2006**, *E62*, o4337.
23. Guo, H. M.; Jian, F. F.; Zhao, P. S.; Zhang, Y. C.; Li, Y. F. *Acta Cryst*. **2007**, *E63*, o215.
24. Fahrni, C. J.; Yang, L. C.; VanDerveer, D. G. *J. Am. Chem. Soc*. **2003**, *125*, 3799.
25. Hunter, R. H.; Haueisen, R. H.; Irving, A. *Angew. Chem. Int. Ed. Engl*. **1994**, *33*, 566.
26. Glusker, J. P.; Lewis, M.; Rossi, M. *Crystal Structure Analysis for Chemistry and Biologists*; VCH: New York, 1994.
27. Olsen, L.; Jorgensen, P. In *Modern Electronic Structure Theory*; World Science: River Edge, NJ, 1995; Vol. 2.
28. Fernando, M.; Claudio, O. A. *Int. J. Quant. Chem*. **103**, *34*, 2005.